Studies on Adsorption of 5-Amino Tetrazole on Silver Nanoparticles by SERS and DFT Calculations

S. Thomas,*,† N. Biswas,‡ S. Venkateswaran,† S. Kapoor,*,‡ S. Naumov,§ and T. Mukherjee‡

Synchrotron Radiation Section, Radiation Chemistry & Chemical Dynamics Division, Bhabha Atomic Research Centre, Trombay, Mumbai 400085, and Leibniz-Institut für Oberflächenmodifizierung, Permoserstrasse 15, D-04318 Leipzig, Germany

Received: July 8, 2005; In Final Form: September 13, 2005

The surface-enhanced Raman scattering (SERS) studies of 5-amino tetrazole (5AT), a tetrazole derivative, in aqueous silver sol at pH ∼ 9 and on deposited colloidal silver films were carried out and compared with the normal Raman spectrum of the molecule. The experimentally observed Raman bands along with their corresponding infrared bands were assigned based on the results of density functional theory (DFT) calculations. The significant changes evidenced between the SERS and the normal Raman spectra combined with the theoretical data obtained for Ag−5AT system demonstrated that the molecule is adsorbed on colloidal Ag particles through the lone pair of electrons of the nitrogen atom. The contribution of the chemical mechanism for the SERS enhancement was proved by the behavior of the electronic absorption spectrum of the Ag colloid upon addition of 5AT. This is further supported by the theoretical calculations that show that the favorable interaction of the frontier orbitals localized on Ag^+ and the negatively charged nitrogen from the tetrazole ring leads to the formation of the stable (up to 130 kJ mol^{-1}) charge-transfer complex. The orientation of the adsorbed species with respect to the metal surface was also predicted by applying the "surface selection rule". In addition, the feasibility of the formation of the polymeric species has also been discussed.

Introduction

Triazole and tetrazole derivatives are known to be corrosion inhibitors and have widespread applications in the surface treatment of metals. A large number of investigations including surface-enhanced Raman scattering (SERS) have been carried out on benzotriazole, in particular, to elucidate the interaction mechanism between the molecule and metal surfaces.[1−6]

SERS is a phenomenon resulting in strongly increased Raman signals from molecules, which have been attached to "rough" metal surfaces or to nanometer-sized metallic colloidal particles.[7,8] Apart from the increased sensitivity in the Raman detection limit, SERS is an effective technique in studying surface−interfacial properties and has been used at the molecular level to investigate and characterize the interaction between the substrate and the adsorbate. Shifts in vibrational frequencies and relative intensities in the spectra of adsorbed molecular species compared with that in solution provide information on the average conformation of the adsorbed molecule and the relative proximity of the different parts of the adsorbed molecule to the surface. The "surface selection rule" of Moskovits and Suh[9−13] based on image dipole field theory[14] has formed the basis for the interpretation of SERS data leading to information on the orientation of the adsorbed molecule relative to the metal surface.

5-Amino tetrazole (5AT), a tetrazole derivative, is also a well-known corrosion inhibitor,[15] but its interaction with the metal surface involving SERS studies is not known. Silver nanoparticles in the form of a colloidal solution are predominantly used to study the SERS of molecules. A SERS substrate in the form of film has potential use and can be tailored for a wide variety of applications involving optical, electronic, and catalytic properties.[16] Hence, it would be worthwhile to study the nature of binding of 5AT on thin films of metal nanoparticles in addition to the silver solid.

In this paper, we have studied the FTIR and Raman spectra of solid 5AT, the Raman spectra of 5AT in aqueous solution (pH ∼ 9), and the SERS spectra in aqueous silver sol and on silver film to investigate the nature of the binding of the molecule with the silver surface and the probable molecular orientation the molecule assumes on the surface. DFT (B3LYP/LANL2DZ) calculations have been carried out for a detailed interpretation of SERS spectra by considering various models of surface complexes where the molecule is bound to surface atoms. The feasibility of the formation of the polymeric species has also been discussed. In addition, we have carried out the DFT calculations to calculate the energies of the amino and imino forms of 5AT, since amino−imino tautomerism has been a subject of several investigations on 5AT.[17−20]

Experiment

Aqueous silver sol was prepared by the reduction of silver nitrate with sodium borohydride using the method of Creighton et al.[21] Water purified by a Millipore system was used for the preparation of the silver sol. Silver coated thin film was prepared by dipping glass slides in a 10^{-2} M solution of $AgNO_3$ in formamide for 2.5 hours, and the preparation and characterization have been discussed elsewhere.[22] The film was then dipped in the aqueous solution of 5AT for 15 min and removed and

---

* To whom correspondence should be addressed. E-mail: sudhirk@apsara.barc.ernet.in (Dr. S. Kapoor); susy@magnum.barc.ernet.in (Ms. S. Thomas). Fax: (+) 91-22-25505151. Tel: (+) 91-22-25590298.

† Synchrotron Radiation Section.

‡ Radiation Chemistry & Chemical Dynamics Division.

§ Leibniz-Institut für Oberflächenmodifizierung, Permoserstrasse 15, D-04318 Leipzig, Germany.

10.1021/jp0537512 CCC: $30.25

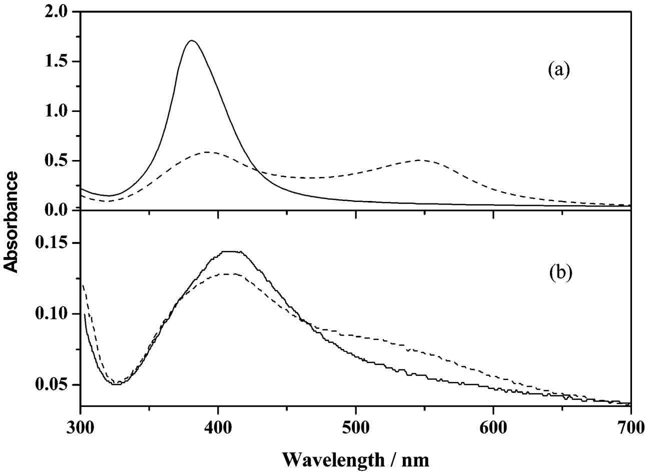

Figure 1. (a) UV−vis spectrum of silver solid (solid line) and with added 5AT (dashed line), and (b) UV−vis spectrum of silver film (solid line) and with added 5AT (dashed line).

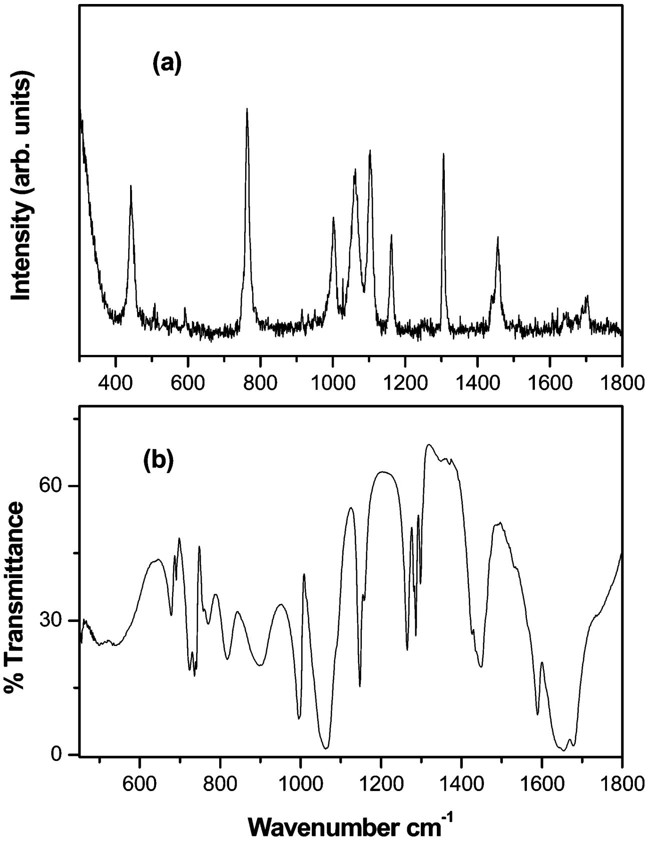

Figure 2. (a) Normal Raman spectrum and (b) FTIR spectrum of 5AT (solid).

dried in air. The UV−vis absorption spectrum was recorded using a Chemito UV2600 spectrophotometer. 5AT and formamide were from Aldrich and Spectrochem, India, respectively.

The Raman spectra of the solid and solution were recorded using a SPEX Ramalog double monochromator (model 1401). The samples were taken in a capillary tube and were excited using the 514.5 nm line of a Coherent Ar^+ laser with a laser power of 100 mW. The spectrometer was operated in the photon counting mode, and a PC based system was used for data acquisition and monochromator control. The SERS spectrum of the film was recorded using the 532 nm line from a diode-pumped Nd^{3+}:YAG laser (SUWTECH laser, model G-SLM-020 from Shanghai Uniwave Technology Co. Ltd.). The laser power used to excite the Raman spectrum was 25 mW. The Raman scattered light was collected at the backscattered geometry and detected using a CCD based, home-built monochromator[23] together with a super notch filter, covering a spectral range of 150−1750 cm^{-1}. The SERS spectrum of the molecule adsorbed on the film was recorded using CCD as the detector to ensure no photodecomposition of the film.

The IR spectrum of 5AT was obtained using a BOMEM DA3.008 model FTIR spectrometer with a KBr beam splitter and MCT detector. Two milligrams of the sample was mixed with 200 mg of pure KBr powder, and a pellet was made. The spectrum was recorded with a 2 cm^{-1} resolution.

Results and Discussion

UV−vis Absorption Spectra. The UV−vis absorption spectra of the silver sol and silver film before and after the addition of 5AT are shown in Figure 1. The absorption spectrum of the silver sol showed a single sharp molar extinction maximum at 380 nm.[24] The yellow sol changed its color to pink after 15 min, and the absorption spectrum showed a second band at about 550 nm with a decrease in the absorbance of the 380 nm band. The new band is attributed to a charge-transfer/aggregate band.[25,26] Since the above band does not show any shift with time, it indicates the origin of a charge-transfer interaction between the molecule and the metal. In the case of the silver film, the surface plasmon band was observed at 405 nm and the charge-transfer band appeared as a shoulder around 520 nm.

Infrared, Raman, and SERS Spectra. The Raman and FTIR spectra of solid 5AT were recorded and are shown in Figure 2 with the frequencies listed in Table 1. The SERS spectrum of 5AT is shown in Figure 3 along with the normal Raman spectrum of the molecule at identical pH. On comparing the spectrum obtained and the data summarized in Table 2, we note drastic changes in the region of 900−1200 cm^{-1} which suggests the existence of a strong interaction between 5AT and the silver surface.

The Raman spectrum of solid 5AT that exists in the monohydrate form is shown in Figure 2a. In the 900−1200 cm^{-1} region, four bands are observed at 998 cm^{-1}, 1157 cm^{-1}, and a doublet comprised of peaks at 1056 and 1098 cm^{-1} and are assigned to the ring stretches and ring bends. The peaks at 1056 and 1098 cm^{-1} also have contributions from the NH_2 rocking mode. A strong peak at 760 cm^{-1} is assigned to the ring in-plane (ip) bend, $N_6C_5N_1$ bend, $N_6C_5N_4$ bend, and H_2O rock, whose normal mode displacement is shown as a footnote (*b*) in Table 1. The peak due to the NH_2 scissoring and C_5N_6 stretching modes are observed as weak bands at 1665 and 1697 cm^{-1}. H_2O scissoring appears at 1635 cm^{-1}. NH_2 rock in combination with ring rock and H_2O rock appears as a strong peak at 442 cm^{-1}. A strong band is observed at 1300 cm^{-1}, which is assigned to the ring NH ip bend and ring stretch. In the IR spectrum of solid 5AT shown in Figure 2b, the ring stretches, with contributions from ring bends, appear as strong bands in the region of 900−1200 cm^{-1}. A strong peak at 1449 cm^{-1} is also assigned to the NH_2 rock, ring stretch, and ring NH ip bend. The NH_2 scissoring with contributions from the C_5N_6 stretch appears as strong peaks at 1651 and 1678 cm^{-1}. The peak assigned to the ring ip bend, $N_6C_5N_1$ bend, $N_6C_5N_4$ bend, and H_2O rock is observed at 770 cm^{-1}. H_2O scissoring appears at 1640 cm^{-1} while the H_2O rock appears at 542 cm^{-1}.

The bands observed in the Raman spectrum of 5AT in the aqueous solution (pH ∼ 9) are weak. A single prominent band

TABLE 1: FTIR, Raman Spectra, and Calculated Frequencies of $5AT\cdot H_2O$ and Their Assignments

		calculated[a]						
Raman cm^{-1}	FTIR cm^{-1}	I	II	III	IV	V	VI	approximate assignments
442 (s)		425	394	376	385	384	427, 418	NH_2 rock, ring rock, H_2O rock
	500 (m,br)							
	542 (m,br)	594		472			591	H_2O rock
	678 (m)	663	677	675	675	675	650	ring tor., oop ring NH bend
	691 (w)	691			679	680	673, 670	oop bend of NH_2, oop bend of H_2O, ring tor.
	724(m)	736	741	739	735	735	746, 738	ring tor.
	736 (m)							
	742 (m)							
760 (s)	770 (m)	744	738	743	738	739	751, 744	(ring ip bend, $N_6C_5N_1$ bend, $N_6C_5N_4$ bend, H_2O rock)[b]
	817 (m)	873		919			845, 805	NH_2 oop, H_2O rock
	899 (m,br)	906	940	953	935	942	934	ring (NN) str., ring NH ip bend, NH_2 rock
998 (m)	997 (s)	999	985	994	971	975	1005	ring str., ring bend, ring NH ip bend
1056 (s)	1062 (s,br)	1034	1028	1022	1043	1044	1058, 1036, 1022	ring str., NH_2 rock
1098 (s)		1099	1056	1044	1033	1034	1099, 1091	NH_2 rock, ring str. ring NH ip bend,
1157 (m)	1147 (s)	1102	1102	1103	1106	1110	1117	ring str., ring bend
	1158 (sh)							
	1265 (s)	1216	1200	1205	1220	1209	1235	
1300 (s)	1286 (s)	1359	1513	1395	1363	1361	1369	ring NH ip bend, ring str.
	1297 (m)							
1433 (sh)	1427 (sh)	1447	1412	1437	1431	1430	1443, 1433	NH_2 rock, ring str., ring NH ip bend
1450 (m)	1449 (s)							
	1590 (m)							
1635 (w)	1640 (s)	1601	1615	1590	1653	1643	1642	H_2O sciss.
1665 (w)	1651 (s)	1654	1647	1637	1641	1640	1677, 1662	NH_2 sciss., N_6C_5 str.
1697 (w)	1678 (s)	1698	1682	1681	1686	1686	1715, 1689	NH_2 sciss., N_6C_5 str.

[a] Calculated unscaled frequencies (B3LYP/LANL2DZ) for various conformers (I−V) of $5AT\cdot H_2O$ and (VI) of $(5AT)_2\cdot H_2O$: w, weak; m, medium; s, strong; br., broad; str., stretch; tor., torsion; sciss., scissoring; ip, in-plane; oop, out-of-plane. [b]

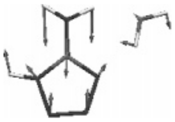

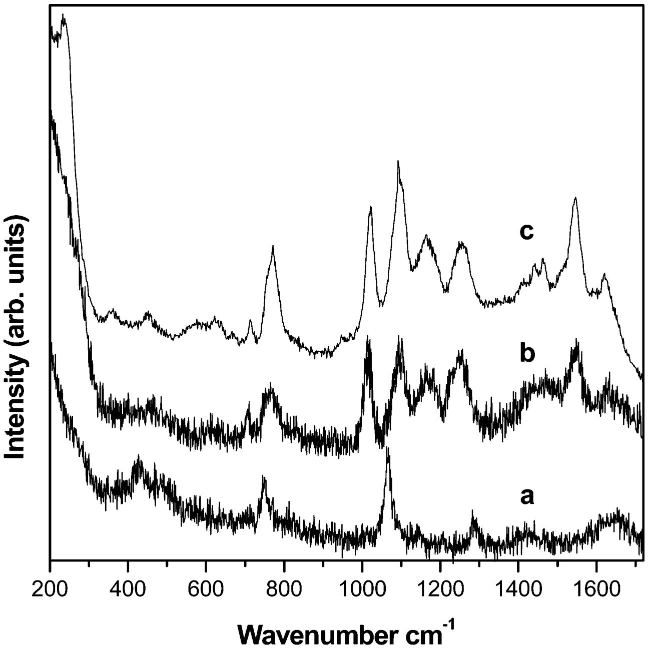

Figure 3. (a) Normal Raman spectrum of alkaline 5AT (10^{-1} M), (b) SERS spectrum of 5AT (10^{-3} M) in silver sol, and (c) SERS spectrum of 5AT on silver film.

at 1061 cm^{-1} attributed to the NH_2 rock, ring stretch, and ring ip bend was observed in the region of 900−1200 cm^{-1}, unlike the four bands seen in the solid state. A moderate intense peak attributed to ring torsion appears at 747 cm^{-1}. The peaks observed in the other regions are weak. The NH_2 scissoring modes (1615 and 1655 cm^{-1}) and the ring stretch at 1417 cm^{-1} appear as weak broad bands. The peak at 1417 cm^{-1} also has a contribution from the NH_2 rock.

In the SERS spectrum of 5AT in the silver sol, strong peaks at 1008, 1090 , 1162, and 1245 cm^{-1} appear in the place of a single, prominent peak at 1061 cm^{-1} observed in aqueous solution. They are the ring stretches and ring ip bend of the molecule that show marked enhancement. The band at 1090 cm^{-1} has a contribution from the NH_2 rock. The broad peak at 1451 cm^{-1} is attributed to the ring stretch and NH_2 rock. The bands at 1628 and 1539 cm^{-1} are attributed to the NH_2 scissoring mode and N_6C_5 stretch with the latter peak having a contribution from the ring stretch as well. The peak that appears at 761 cm^{-1} in the SERS spectrum is assigned to the ring ip bend, $N_6C_5N_1$ bend, and $N_6C_5N_4$ bend as shown in the normal mode displacement in the footnote (*b*) of Table 2 and is similar to the mode at 760 cm^{-1} in the Raman spectra of the solid. A peak that was not observed in the normal Raman spectrum appears at 704 cm^{-1}, which is assigned to the ring torsion. The SERS spectrum of the 5AT molecule on silver film also showed similar features as discussed above but with additional peaks observed in the region below 700 cm^{-1} which are assigned to the out-of-plane (oop) modes. The peaks at 668 and 360 cm^{-1} correspond to the ring torsions. A distinct peak observed at 238 cm^{-1} is assigned to the Ag−N stretch, while in the SERS spectrum of 5AT in silver sol it is seen as a weak, broad feature.

The appearance of new bands and the relative enhancements observed in SERS with respect to the normal Raman bands play an important role for investigating the adsorption mechanism because they are closely related to the atoms directly bound to the surface. Normal modes of adsorbed molecules involving changes in molecular polarizability with a component perpen-

TABLE 2: Normal Raman, SERS Spectral Data, and Calculated Raman Active Frequencies for 5AT and the Ag−5AT Complex (structures II and III) in Water Along with Their Band Assignments

Raman cm^{-1}	calcd.[a]	approximate assignments	SERS (sol) cm^{-1}	SERS (film) cm^{-1}	struture II[a]	structure III[a]	approximate assignments
				238 (w)	210	209	AgN str.
				360 (w)	319	326	NH_2 wag, ring tor.
427 (w)	369	NH_2 rock, ring rock	431 (w)	450 (w)	412	416	NH_2 rock, ring rock
				571 (w)			
				627 (w)	682	672	ring tor.
			704 (w)	712 (w)	745	702	ring tor.
747 (m)	742	ring tor.	761 (m)	772 (s)	743	750	(ring ip bend, $N_6C_5N_1$ bend, $N_6C_5N_4$ bend)[b]
			1008 (s)	1022 (s)	959	969	ring ip bend, ring str.
	1030	NH_2 rock,			1013	1015	NH_2 rock,
1061 (s)	1050	ring ip bend,	1090 (s)	1095 (s)	1023	1026	ring ip bend,
	1084	ring str.			1079	1098	ring str.
1133 (w)	1131	ring str., ring bend	1162 (s)	1167 (s)	1115	1119	ring str., ring ip bend
1282 (w)			1245 (s)	1257 (s)	1173	1214	ring str., ring ip bend
1417 (w,br.)	1375	ring str., NH_2 rock	1451 (w)	1447 (m)	1385	1369	ring str., NH_2 rock
				1511 (m)			
1615 (w)	1575	NH_2 sciss., N_6C_5 str., ring str.	1539 (m)	1545 (s)	1574	1569	NH_2 sciss., N_6C_5 str., ring str.
1655 (w)	1684	NH_2 sciss., N_6C_5 str.	1628 (w)	1621(m)	1621	1623	NH_2 sciss., N_6C_5 str.

[a] Calculated unscaled frequencies for 5AT and 5AT−Ag in water (B3LYP/LANL2DZ//SCRF = CPCM): w, weak; m, medium; s, strong; br., broad; str., stretch; tor., torsion; sciss., scissoring; ip, in-plane; oop, out-of-plane. [b]

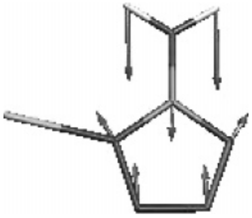

dicular to the surface are subject to the greatest enhancement according to “surface selection rules”. The in-plane modes are significantly enhanced in the SERS spectra of both the sol and the film whereas more ring torsional modes are observed in the film compared to that of sol. The appearance of the low-frequency mode at 238 cm^{-1} and the enhancements seen in the ip and oop modes suggest that the molecule becomes adsorbed onto the silver surface through the nitrogen atom of the molecule with the molecular plane tilted with respect to the surface. The tilt seems to be greater in the case of the 5AT molecule adsorbed onto the silver film with a molecular plane tending toward a flat orientation.

Computational Results and Discussion

Geometry optimization and frequency analysis were performed for 5AT using the density functional theory (DFT) with a B3LYP functional[27−29] and LANL2DZ basis set using the Gaussian 98 program.[30] Frequency calculations were used to characterize the stationary points and to calculate the IR and Raman active harmonic frequencies. The LANL2DZ basis set, which makes use of ECP pseudopotentials for silver atoms, was used for calculations of the Ag(I)−5AT$^{(-)}$ complexes. As was already shown by the study of the Ag(I)−benzotriazole complexes,[2] the calculated Raman active frequencies (both in a vacuum and water) with the LANL2DZ basis set agree well with those calculated with the 6-31++G(d,p) basis set, which is sufficient for the calculations of geometrical parameters and harmonic frequencies of such ring structures containing heteroatoms as a pyrazolide anion and pyrimidine bases.[31] Consequently, the LANL2DZ basis set was used for the calculations of the 5AT and Ag(I)−5AT$^{(-)}$ complexes.

The amino and imino forms for 5AT were optimized, and the amino form was found to be more stable (40 kJ mol^{-1}) compared to the imino form. This study corroborates with the IR and Raman study of 5AT·H_2O, 5AT, and 5AT in aqueous solution by Bigotto et al., which shows that the molecule exists only in the amino form both in the solid state and in the aqueous solution.[15] Various possible conformers of 5AT·H_2O (simplified model containing one 5AT and one H_2O molecule) were computed and their energies optimized (the energies in kJ mol^{-1} are relative to the most stable conformer I (0), II (16), III (15), IV (37), and V (38)). The optimized structures of these conformers are shown in Figure 4(I−V). Frequency calculations were carried out for all the conformers and are listed in Table 1. The crystal structure of 5AT·H_2O shows that four 5AT molecules are bound to one molecule of H_2O.[32] The five conformers of 5AT·H_2O obtained from our calculations cover most of the H-bonded interactions seen in the crystal structure. To our simplified model, a second 5AT molecule was also added (Figure 4 (VI)) to see the extent of variation in the modes. It is to be noted that the addition of a second 5AT molecule to the simplified model showed not much variation in the calculated frequencies.

In aqueous solution (pH ∼ 9), 5AT exists in its deprotonated form as the anion 5AT$^{(-)}$. The molecular structure and the electron density distribution of the radicals and radical ions of pyrimidine-type bases are strongly influenced by a surrounding in aqueous solution.[33−35] Moreover, the calculated Raman active frequencies in water (SCRF = CPCM) satisfactorily reproduce the experimental normal Raman spectra of the benzotriazole anion.[2] Hence, to take into account the influence of the solvent (water) on the molecular structure of 5AT$^{(-)}$, geometry optimizations were carried out in water using a SCRF = CPCM polarized continuum model.[36,37]

The deprotonation of 5AT in water can occur either from the ring or from the NH_2 group. According to the calculations,

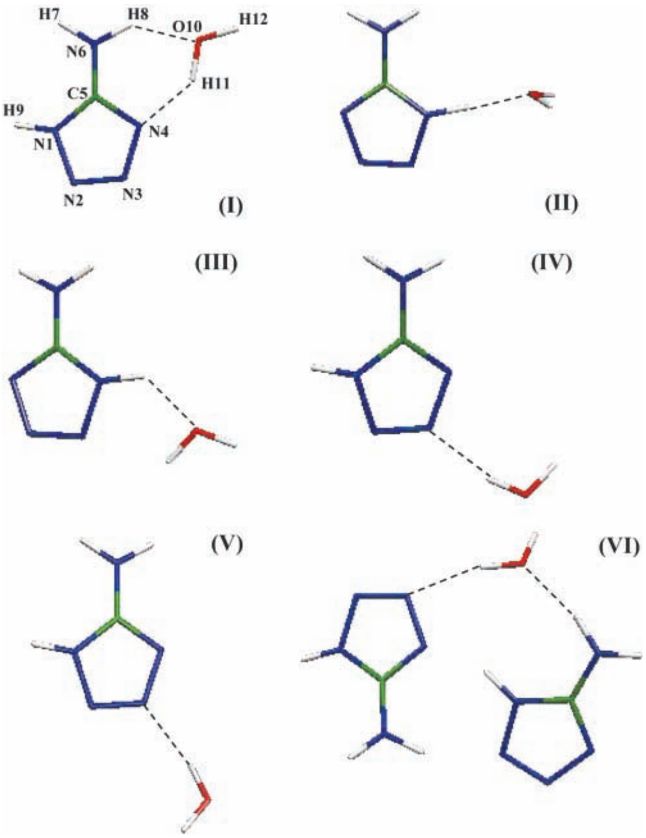

Figure 4. Optimized structures of $5AT\cdot H_2O$ (I−V) and $(5AT)_2\cdot H_2O$ (VI) calculated using B3LYP/LANL2DZ.

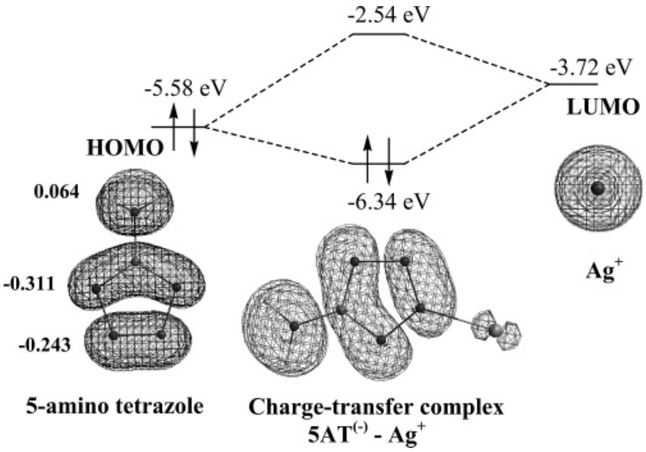

Figure 5. Frontier molecular orbitals scheme of charge-transfer complex formation of $5AT^{(-)}-Ag^+$ and calculated Mulliken charges on N-atoms (with H-atom summed to a heavy atom) of $5AT^{(-)}$. Mulliken charge shift in the complex (ΔQ) is equal to 0.3 (B3LYP/LANL2DZ//SCRF = CPCM, isocontour = 0.02).

deprotonation from the molecular ring is energetically more favorable (58.5 kJ mol^{-1} at the B3LYP/6-31++G(d,p) level). The molecular structure of $5AT^{(-)}$ is planar, and the calculated harmonic frequencies of isolated $5AT^{(-)}$ are in reasonable agreement with the experimental data and are listed in Table 2.

To determine the most plausible model for the $Ag(I)-5AT^{(-)}$ complex, the electronic structure of $5AT^{(-)}$ was analyzed. It is established that an effective SERS enhancement is detected when the molecule is able to form a chemical bond with the surface. According to frontier orbital theory,[38−40] the chemical reactivity for two molecules in their ground states depends mainly on two factors: an electrostatic interaction approximated by atomic charges and a frontier orbital interaction. The reaction proceeds in a way to produce the most favorable interaction energy. Frontier orbital theory supplies an additional assumption that the reaction depends on the interactions between only the highest occupied molecular orbital (HOMO) on one molecule and the lowest unoccupied molecular orbital (LUMO) of the other (and conversely), which have the smallest energy separation. The analysis of electronic structure of the reaction partner (Figure 5) shows that, due to the smallest energy gap between MOs, the most favorable interaction should occur between the HOMO of the electron donor ($5AT^{(-)}$) and LUMO of the electron acceptor (Ag$^+$).

However, as can be seen in Figure 5, the electron density from the HOMO of $5AT^{(-)}$ is distributed uniformly throughout the molecule with a slightly larger electron density in position $N_{2,3}$ than that in $N_{1,4}$, which should lead to the preference of position $N_{2,3}$ due to the strongest frontier orbital interaction with Ag$^+$. In contrast, the calculated negative charge is slightly larger in position $N_{1,4}$ than $N_{2,3}$ as shown in Figure 5. This should favor position $N_{1,4}$ due to a stronger Coulombic interaction. The calculations of possible structures of the $Ag(I)-5AT^{(-)}$ complexes (Figure 6) show very large stabilization energies in all cases (up to 130 kJ mol^{-1}). The interaction between Ag$^+$ and $5AT^{(-)}$ has a strong charge-transfer character with a positive charge shift from Ag$^+$ to $BTA^{(-)}$ up to 0.300 e in water (0.435 e in a vacuum). The $Ag(I)-5AT^{(-)}$ complex bonded through $N_{1,4}$ (structure II) is only 6 kJ mol^{-1} more stable than that through $N_{2,3}$ (structure III). That is in agreement with the nearly uniform electron distribution and slightly larger negative charge on $N_{1,4}$. It should be mentioned that the HOMO has a large electron density on the N_6 atom due to a lone pair, which should lead to strong frontier orbital interaction. However, the $Ag(I)-5AT^{(-)}$ complex through N_6 is not stable by geometry optimization and transforms to a more energetically stable complex through N_1. This instability of the complex through N_6 is caused apparently by a positive charge on the NH_2 group. Hence, both forms of the $Ag(I)-5AT^{(-)}$ complexes II and III are considered. The calculated Raman active frequencies for complexes II and III and their assignments are given in Table 2. These are in reasonable agreement with the SERS spectra of 5AT on the silver surface. The calculated vibrations of the $Ag(I)-5AT^{(-)}$ complex in water and in a vacuum vary within a few cm^{-1}, and hence, the frequencies in a vacuum are not included in the table.

In our earlier studies on the Ag(I)−benzotriazole complexes,[2] the possibility of building the polymeric metal−benzotriazole complex was discussed. To study possible polymeric metal−$5AT^{(-)}$ complexes, calculations on different polymeric structures (see Figure 6) were carried out. The polymeric process seems energetically favorable. Complexes II and III can react with comparable reaction enthalpy with $Ag^{(+)}$ to build structures IV, V, and VI with complex V being energetically slightly more stable. Complex V can be formed from structures II and III and is thus statistically most probable. Both $Ag(I)-5AT^{(-)}$ complexes II and III can also react (reaction enthalpy of 155 kJ mol^{-1}) with $5AT^{(-)}$ and build polymeric structure VII. Structures VII and V can also lead to the polymeric structure VIII as shown in the Figure 6.

It is worth mentioning that independent of the reaction pathways from I to VIII of polymer chain formation, the calculated mean stabilization energy per of the $Ag(I)-5AT^{(-)}$ bond is 128 kJ mol^{-1}. The driving force has strong charge-transfer character with a very large positive charge shift from

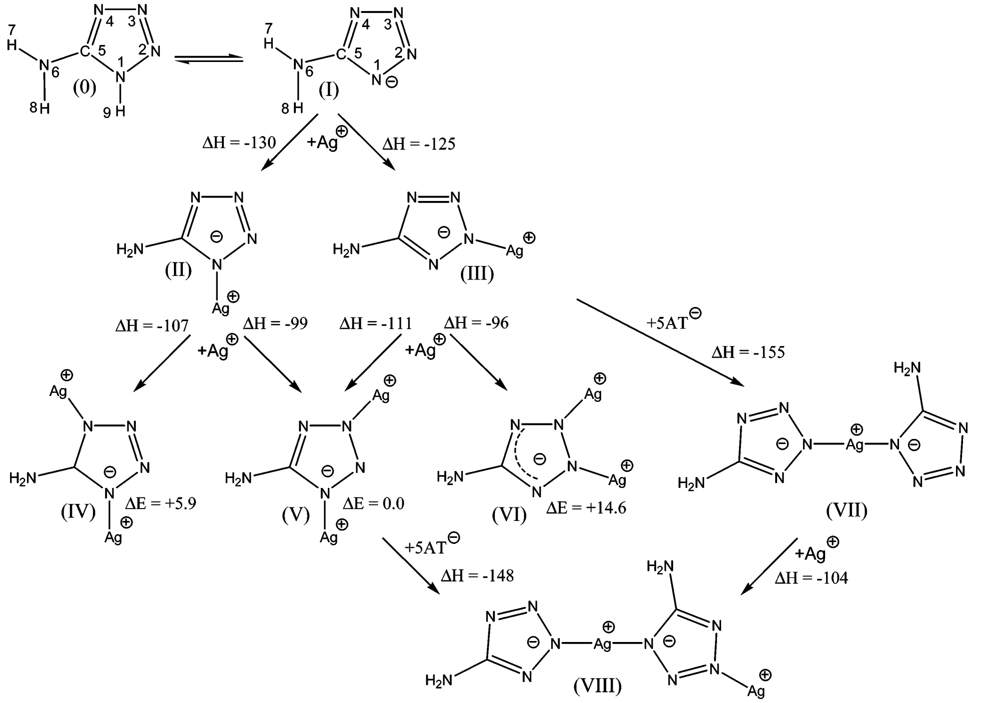

Figure 6. Formation scheme of the possible complexes of $5AT^{(-)}$ with $Ag^{(+)}$, ΔH (kJ mol^{-1}) is the reaction enthalpy and ΔE (kJ mol^{-1}) is the relative stability of the complexes (IV, V, and VI) as calculated in water (B3LYP/LANL2DZ//SCRF = CPCM).

Ag^+ to $5AT^{(-)}$ (about 0.30 e if silver is connected to one N atom and up to 0.55 e if the silver atom is connected to two N atoms).

Conclusion

Raman, FTIR, SERS spectrum (Ag sol and Ag film), and theoretical studies of 5AT have been investigated. The calculations show that 5AT in the solid state exists in the amino form. In the SERS spectrum of 5AT in Ag sol (pH ~ 9) and on Ag film, similar features were observed with significant enhancement seen in the in-plane ring vibrations and a few out-of-plane ring vibrations. By comparing the normal Raman spectrum to the SERS spectrum and also considering the “surface selection rules” applied to the enhanced bands, it is deduced that the molecule interacts with the silver surface through the nitrogen atom of the 5AT molecule and assumes a tilted orientation. In the case of the SERS spectrum on the Ag film, additional ring torsional modes were also observed, suggesting more tilt in the molecular plane tending toward a flat orientation on the surface. DFT (B3LYP/LANL2DZ) calculations support the experimental observation that the 5AT molecule binds to silver nanoparticles through the nitrogen atom of the tetrazole ring and forms the Ag(I)−5AT complex. The favorable interaction of the frontier orbitals localized on Ag^+ and the negatively charged nitrogen from the tetrazole ring leads to the formation of the stable (up to 130 kJ mol^{-1}) charge-transfer complex. The frequencies of the stable surface complexes have been calculated and compared with the experimental values. The formation of the polymeric species was shown to be energetically favorable since there is a calculated mean gain in energy of up to 128 kJ mol^{-1} for each new Ag−N bond.

Acknowledgment. The authors thank Dr. T. Sakuntala and Dr. S.K. Deb of the Synchrotron Radiation Section, BARC, for helping us to record the SERS spectra of the thin films.

References and Notes

(1) Thomas, S.; Venkateswaran, S.; Kapoor, S.; D′Cunha, R.; Mukherjee, T. *Spectrochim. Acta, Part A* **2004**, *60*, 25.

(2) Naumov, S.; Kapoor, S.; Thomas, S.; Venkateswaran, S.; Mukherjee, T. *J. Mol. Struct. (THEOCHEM)* **2004**, *685*, 127.

(3) Pergolese, B.; Muniz-Miranda, M.; Bigotto, A. *J. Phys. Chem. B* **2004**, *108*, 5698.

(4) Tornkvist, C.; Thierry, D.; Bergman, J.; Leidberg, B.; Leygraf, C. *J. Electrochem. Soc.* **1989**, *136*, 58.

(5) Rubim, J. C.; Gutz, I. G. R.; Sala, O.; Oriville-Thomas, W. J. *J. Mol. Struct.* **1983**, *100*, 571.

(6) Mansfeld, F.; Smith, T. *Corrosion* **1973**, *29*, 105.

(7) Chang, R. K., Furtak, T. E., Eds. *Surface Enhanced Raman Scattering*; Plenum: New York, 1982.

(8) Moskovits, M. *Rev. Mod. Phys.* **1985**, *57*, 783.

(9) Moskovits, M.; Suh, J. S. *J. Phys. Chem.* **1988**, *92*, 6327.

(10) Moskovits, M.; Suh, J. S. *J. Phys. Chem.* **1984**, *88*, 5526.

(11) Moskovits, M.; Suh, J. S. *J. Phys. Chem.* **1984**, *88*, 1293.

(12) Moskovits, M.; Suh. J. S. *J. Chem. Phys.* **1982**, *77*, 4408.

(13) Moskovits, M.; Suh, J. S. *J. Am. Chem. Soc.* **1985**, *107*, 6826.

(14) Allen, C. S.; Van Duyne, R. P. *Chem. Phys. Lett.* **1979**, *63*, 455.

(15) Grigorev V. P.; Ekilik, G. N.; Ekilik, V. V. Selection of iron corrosion inhibitors in acid media. *Ingibirovanie Passivirovanie Met.* 39; CHAB 91, 16545q, in Russian, 1976.

(16) Ung, T.; Giersig, M.; Dunstan, D.; Mulvaney, P. *Langmuir* **1997**, *13*, 1773.

(17) Murphy, D. B.; Picard, J. P. *J. Org. Chem.* **1954**, *19*, 1807.

(18) Jonassen, H. B.; Paukert, T.; Henry, R. A. *Appl. Spectrosc.* **1967**, *21*, 89.

(19) Nelson, J. H.; Baglin, F. G. *Spectrosc. Lett.* **1972**, *5*, 101.

(20) Bigotto, A.; Castellani, G. *J. Raman Spectrosc.* **1984**, *15*, 232.

(21) Creighton, J. A. In *Spectroscopy of Surfaces;* Hester, R. E., Clark, R. J. H., Eds.; Wiley: New York, 1988; Vol. 37.

(22) Sarkar, A.; Kapoor, S.; Mukherjee, T. *J. Colloid Interface Sci.* **2005**, *287*, 496; *J. Phys. Chem. B* **2005**, *109*, 7698.

(23) Roy, A. P.; Deb, S. K.; Rekha, M. A.; Sinha, A. K. *Ind. J. Pure Appl. Phys.* **1992**, *30*, 724.

(24) Creighton, J. A. In *Surface Enhanced Raman Scattering*; Chang, R. K., Furtak, T. E., Eds.; Metal Colloids, Plenum Press: New York, 1982; pp 315−337.

(25) Yamada, H.; Nagata, H.; Toba, K.; Nakao, Y. *Surf. Sci.* **1987**, *182*, 269. Yamada, H. In *Vibrational Spectra and Structure*; Bist, H. D., Durig, J. R., Sullivan, J. F., Eds.; Elsevier: Amsterdam, The Netherlands, 1989; Vol. 17A, p 391. Sanchez-Cortes, S.; Gracia-Ramos, J. V.; Morcillo, G.; Tinti, A. *J. Colloid Interface Sci.* **1995**, *175*, 358.

(26) Creighton, J. A.; Blatchford, C. G.; Albrecht, M. G. *J. Chem. Soc., Faraday Trans. 2* **1979**, *75*, 790. Blatchford, C. G.; Campbell, J. R., Creighton, J. A. *Surf. Sci*. **1982**, *120*, 435.

(27) Becke, A. D. *J. Chem. Phys.* **1993**, *98*, 5648.

(28) Becke, A. D. *J. Chem. Phys.* **1996**, *104*, 1040.

(29) Lee, C.; Yang, W.; Parr, R. G. *Phys. Rev. B* **1987**, *37*, 785.

(30) Frisch, M. J.; Trucks, G. W.; Schlegel, H. B.; Scuseria, G. E.; Robb, M. A.; Cheeseman, J. R.; Zakrzewski, V. G.; Montgomery, J. A., Jr.; Stratmann, R. E.; Burant, J. C.; Dapprich, S.; Millam, J. M.; Daniels, A. D.; Kudin, K. N.; Strain, M. C.; Farkas, O.; Tomasi, J.; Barone, V.; Cossi, M.; Cammi, R.; Mennucci, B.; Pomelli, C.; Adamo, C.; Clifford, S.; Ochterski, J.; Petersson, G. A.; Ayala, P. Y.; Cui, Q.; Morokuma, K.; Malick, D. K.; Rabuck, A. D.; Raghavachari, K.; Foresman, J. B.; Cioslowski, J.; Ortiz, J. V.; Stefanov, B. B.; Liu, G.; Liashenko, A.; Piskorz, P.; Komaromi, I.; Gomperts, R.; Martin, R. L.; Fox, D. J.; Keith, T.; Al-Laham, M. A.; Peng, C. Y.; Nanayakkara, A.; Gonzalez, C.; Challacombe, M.; Gill, P. M. W.; Johnson, B. G.; Chen, W.; Wong, M. W.; Andres, J. L.; Head-Gordon, M.; Replogle, E. S.; Pople, J. A. *Gaussian 98*, revision A.11; Gaussian, Inc.: Pittsburgh, PA, 1998.

(31) Cardini, G.; Muniz-Miranda, M. *J. Phys. Chem. B* **2002**, *106*, 6875.

(32) Bray, D. D.; White J. G. *Acta Crystallogr*. **1979**, *B35*, 3089.

(33) Naumov, S.; Barthel, A.; Reinhold, J.; Dietz, F.; Geimer, J.; Beckert, D. *Phys. Chem. Chem. Phys.* **2000**, *2*, 4207.

(34) Naumov, S.; Hildenbrand, K.; von Sonntag, C. *J. Chem. Soc., Perkin Trans*. **2001**, *2*, 1648.

(35) Naumov, S.; Reinhold, J.; Beckert, D. *Phys. Chem. Chem. Phys.* **2003**, *5*, 64.

(36) Klamt, A.; Schüürmann, G. *J. Chem. Soc., Perkin Trans.* **1993**, *2*, 799.

(37) Rega, N.; Cossi, M.; Barone, V. *Chem. Phys.* **1996**, *105*, 11060.

(38) Klopman, G. *J. Am. Chem. Soc.* **1968**, *90*, 223.

(39) Salem, L. *J. Am. Chem. Soc*. **1968**, *90*, 543

(40) Fleming, I. *Frontier Orbitals and Organic Chemical Reactions*; Wiley and Sons: London, 1976; Vol. 34.